Epitope Mapping of Herpes Simplex Virus Type 2 gH/gL Defines Distinct Antigenic Sites, Including Some Associated with Biological Function

Tina M. Cairns, Marie S. Shaner, Yi Zuo, Manuel Ponce-de-Leon, Isabelle Baribaud, Roselyn J. Eisenberg, Gary H. Cohen and J. Charles Whitbeck

J. Virol. **2006, 80(6):2596. DOI: 10.1128/JVI.80.6.2596-2608.2006.**

JOURNAL OF VIROLOGY, Mar. 2006, p. 2596–2608 Vol. 80, No. 6
0022-538X/06/$08.00+0 doi:10.1128/JVI.80.6.2596–2608.2006

Epitope Mapping of Herpes Simplex Virus Type 2 gH/gL Defines Distinct Antigenic Sites, Including Some Associated with Biological Function

Tina M. Cairns,[1]† Marie S. Shaner,[1]† Yi Zuo,[1] Manuel Ponce-de-Leon,[1] Isabelle Baribaud,[1] Roselyn J. Eisenberg,[2] Gary H. Cohen,[1] and J. Charles Whitbeck[1,2]*

Department of Microbiology, School of Dental Medicine,[1] and Department of Pathobiology, School of Veterinary Medicine,[2] University of Pennsylvania, Philadelphia, Pennsylvania 19104

Received 24 October 2005/Accepted 16 December 2005

The gH/gL complex plays an essential role in virus entry and cell-cell spread of herpes simplex virus (HSV). Very few immunologic reagents were previously available to either identify important functional regions or gain information about structural features of this complex. Therefore, we generated and characterized a panel of 31 monoclonal antibodies (MAbs) against HSV type 2 (HSV-2) gH/gL. Fourteen MAbs bound to a conformation-dependent epitope of the gH2/gL2 complex, and all blocked virus spread. The other 17 MAbs recognized linear epitopes of gH (12) or gL (5). Interestingly, two of the gL MAbs and six of the gH MAbs were type common. Overlapping synthetic peptides were used to map MAbs against linear epitopes. These data, along with results of competition analyses and functional assays, assigned the MAbs to groups representing eight distinct antigenic sites on gH (I to VIII) and three sites on gL (A, B, and C). Of most importance, the MAbs with biological activity mapped either to site I of gH2 (amino acids 19 to 38) or to sites B and C of gL2 (residues 191 to 210). Thus, these MAbs constitute a novel set of reagents, including the first such reagents against gH2 and gL2 as well as some that recognize both serotypes of each protein. Several recognize important functional domains of gH2, gL2, or the complex. We suggest a common grouping scheme for all of the known MAbs against gH/gL of both HSV-1 and HSV-2.

Four glycoproteins (gB, gD, and gH/gL) as well as a gD-binding cellular receptor are required for entry of most alphaherpesviruses, including herpes simplex virus (HSV), pseudorabies virus, and bovine herpesvirus type 1 (36). Although gL shares little amino acid identity across herpesviruses, the gH/gL heterodimer is highly conserved and essential for virus-cell and cell-cell fusion (20, 32, 34). It is not clear how herpesvirus glycoproteins, singly or in combination, mediate fusion. A recent report suggests that gH is the HSV fusion protein (16), but a variety of other studies have shown that gB, gL, and gD are also essential for both virus-cell and cell-cell fusion (27, 33, 38). Although the crystal structure of HSV gD in complex with one of its receptors (HVEM; also called HveA) has been solved (6, 33), the three-dimensional structure of gB is still in a rudimentary stage (E. Heldwein, personal communication) and that of gH/gL has not yet been solved.

Using a genetic approach, a hypothetical disulfide bond structure for HSV type 2 (HSV-2) gH has been proposed (5). Cysteines at positions 2 (residue 258) and 4 (residue 429) are thought to constitute a disulfide-bonded pair (C2-C4), while gH2 C1 (residue 90) is unbound. HSV-1 gH contains one more cysteine in its ectodomain than gH2 (at position 3, residue 404); it is unclear if gH1 C1 remains free or is the disulfide bond partner of gH1 C3. Genetic studies have also suggested disulfide bonds between cysteines 5 and 6 (residues 554 and 589) and cysteines 7 and 8 (residues 652 and 706) (5, 32).

The N- and C-terminal halves of gH comprise separate structural and functional segments (2, 4, 14); indeed, none of the proposed disulfide bonds connect these two domains (5). Residues required for gL binding are located within an N-terminal segment, between residues 19 and 323 (4, 32, 40). Amino acids important for membrane fusion have been identified that are distal to residue 652 (5, 14). However, the C-terminal segment is unable to support cell-cell fusion when expressed as part of a gD/gH chimera (4). This finding suggests that a functional domain may also reside in the N-terminal segment. Indeed, recent studies have indicated the presence of one or more potential fusion peptides in this region of gH of HSV-1 and human cytomegalovirus (15–17, 25).

Although gH1 and gH2 are 80% identical in amino acid sequence, differences between the two proteins have been detected. For example, mutation of gH2 cysteines 7 and/or 8 to serine has no effect on cell-cell fusion mediated by HSV-2 glycoproteins, but similar substitutions in gH1 impair fusion mediated by HSV-1 glycoproteins (5). Mutation of gH2 C2 also impairs the ability of gH2 to function with gL1. However, the same mutation in gH1 has no effect, suggesting structural differences in the N-terminal region between the two serotypes of gH.

A limited number of monoclonal antibodies (MAbs) to gH1/gL1 are available. Two linear epitopes were coarsely mapped to residues 19 to 276 and 475 to 648 of gH1 (32, 35). In addition, both neutralizing and nonneutralizing MAbs bind within amino acids 19 to 276. Several gL1-specific antibodies map to a region between residues 168 and 224 (30, 32). Although all of the MAbs affect cell-cell spread, none neutralize the virus. The type-specific MAb LP11 recognizes conformation-dependent epitopes of the gH1/gL1 complex and has neutralizing activity (3, 18). No type-specific MAbs have heretofore been described for HSV-2 gH or gL.

In contrast, a large panel of type-specific and type-common MAbs to gD led to a detailed antigenic map (7, 10, 21, 24, 41)

* Corresponding author. Mailing address: Department of Microbiology, School of Dental Medicine, University of Pennsylvania, Philadelphia, PA 19104. Phone: (215) 898-6553. Fax: (215) 898-8385. E-mail: whitbeck@biochem.dental.upenn.edu.

† T.M.C. and M.S.S. contributed equally to this work.

that proved to be a major asset in interpreting the validity of its three-dimensional structure (6). Using this approach as a precedent, we prepared a panel of MAbs to gH2/gL2 and characterized their properties. Twenty-three of 31 MAbs were type 2 specific, including six that recognized only gH2 and three that recognized only gL2. Interestingly, eight type-common MAbs were isolated, with six against gH and two against gL. A variety of tests were used to map specific MAb binding domains on both gH and gL. The MAbs were further tested in virus neutralization, cell-cell fusion, and plaque size reduction assays. We pinpointed two linear regions of gH and gL, as well as a conformation-dependent site on the gH2/gL2 complex, that were important for function.

MATERIALS AND METHODS

Viruses and cells. African green monkey kidney (Vero) cells were grown in Dulbecco modified Eagle medium (DMEM) containing 5% fetal bovine serum (FBS). Vero cells were infected with HSV-2 (strain 333) and then lysed for use in immunoprecipitation assays (see below). Hybridoma cells were cultured in Kennett's HY complete medium, consisting of DMEM supplemented with 10% NCTC-109 (Gibco), 20% FBS, 1× OPI (Gibco), 50 μM hypoxanthine, 8 μM thymidine, 2 mM L-glutamine, and 3% hybridoma cloning factor (Bio Veris). For the fusion assay, CHOK1 and CHO-A12 cells (a gift of P. G. Spear) were grown in F12 medium containing 10% FBS. CHO-A12 medium also contained 250 μg/ml G418.

Hybridoma selection and IgG purification. Mice were subcutaneously inoculated five times with 50 μg per injection of purified gH2t/gL2. Soluble gH2t/gL2 was generated by large-scale transfection of 293T cells with plasmids pCW333 (encoding gH2t) and pWF318 (encoding full-length gL2) (5), using the Gene Porter method (Gene Therapy Systems, Inc.). At 1 day posttransfection, the growth medium was replaced with 0.5% fetal bovine serum-$CaCl_2$-OptiMEM. For CHL1-16, gH2t/gL2 was purified from the culture medium by nickel chelation chromatography; for CHL17-43, gH2t/gL2 was purified using a CHL2 MAb affinity column. In each case, the protein was emulsified in Freund's complete adjuvant at a 1:1 ratio for the first injection. Animals were boosted three times at 3-week intervals. A final boost of 5 μg was given intravenously in the absence of adjuvant, 3 days prior to fusion. Hybridoma fusion was performed by a standard procedure (8). An enzyme-linked immunosorbent assay (ELISA) was used to identify hybridomas secreting anti-gH2/gL2 antibodies. For the ELISA, 96-well plates were coated with 4 μg/ml of purified gH2t/gL2, blocked with phosphate-buffered saline (PBS) containing 0.1% Tween 20 (PBS-T) and 5% milk, and then incubated with 100 μl of hybridoma supernatant for 1 h. Hybridoma cells were subcloned twice from isolated colonies grown under a soft agar overlay. Immunoglobulin G (IgG) antibodies were purified from mouse ascites, using HiTrap protein G columns as specified by the manufacturer (Amersham Pharmacia). IgGs were eluted using 2.5 ml of 0.1 M glycine (pH 2.7) and dialyzed against PBS. An anti-tetrahistidine MAb was purchased from QIAGEN, Inc.

Western blotting and immunoprecipitation. Purified gH2t/gL2 complex was separated by electrophoresis on a 10% sodium dodecyl sulfate (SDS)-polyacrylamide gel under denaturing conditions. Separated proteins were transferred to nitrocellulose, and the membrane was cut into strips. Each strip was probed with one of our panel of MAbs to test for gH or gL binding. This procedure was then repeated using purified gH1t/gL1 (32). The gH2/gL2 polyclonal antibody (PAb) R176 (5) was used as a positive control, and the anti-Myc MAb 9E10 (11) was used as a negative control.

The MAbs were also tested for the ability to immunoprecipitate gH2/gL2 from HSV-2-infected cell extracts. Cells were lysed in a buffer consisting of 10 mM Tris, pH 8, 150 mM NaCl, 10 mM EDTA, 1% NP-40, 0.5% deoxycholic acid, and 1 mM phenylmethylsulfonyl fluoride. Cell extracts were mixed with binding buffer (29) and incubated with MAb for 18 h at 4°C. Proteins were precipitated with protein A-agarose beads (Gibco BRL) for 2 h at 4°C, separated by electrophoresis on a 10% SDS-polyacrylamide gel, and detected by Western blotting with R176.

Peptide mapping. (i) Peptide synthesis. Synthetic 20-mer peptides were purchased from Mimotopes Pty. Ltd. (Melbourne, Australia). The peptides covered the entire ectodomain of gH or gL and overlapped each other by 11 amino acids, with the exception of the last peptides in both the gH and gL sets. Biotin was included at the N terminus of each peptide during synthesis to facilitate binding to streptavidin. Peptides were dissolved in a solution of 10% acetic acid and 20% acetonitrile.

(ii) Epitope mapping with ELISA. Fifty microliters of an approximately 1 μM concentration (in PBS) of each peptide was placed in each well of a 96-well Reacti-bind high-binding-capacity streptavidin-coated plate (Pierce) and incubated for 1 h. The plate was then blocked with 200 μl of 5% milk–PBS-T for 30 min and probed with 50 μl of 20 μg/ml MAb for 1 h in milk–PBS-T. All steps were performed at room temperature. Bound IgG was visualized with goat anti-mouse IgG–horseradish peroxidase (HRP).

RT-PCR. Antibodies that bound noncontiguous peptides were screened by reverse transcription-PCR (RT-PCR) to ensure their clonality. RNAs were extracted from IgG-producing hybridoma cells using an RNeasy mini kit (QIAGEN). cDNAs were generated by reverse transcription using an Omniscript RT kit (QIAGEN) per the manufacturer's protocol. For PCR amplification of the cDNA, primers specific to the kappa light chain were used (39), since this isotype was present in all monoclonal antibodies tested (mouse monoclonal antibody isotyping kit; Amersham Biosciences). PCR conditions were as follows: initial denaturation at 94°C for 3 min, followed by 30 cycles of 1-min steps of 94°C, 45°C, and 72°C and ending with an extension step at 72°C for 10 min (39). Buffer and nucleotides were removed from the PCR products using Geneclean spin columns (Qbiogene). PCR products were eluted in 40 μl of elution solution, 1 μl of which was used for DNA sequencing (University of Pennsylvania DNA sequencing facility).

MAb binding competition by ELISA. An ELISA plate was coated for 2 h with 5 μg/ml of purified gH2t/gL2 diluted in PBS. The plate was then washed with PBS-T and incubated in milk–PBS-T for 1 h to block any remaining protein binding capacity. After the blocking step, individual wells were incubated for 2 h with 50 μg/ml of CHL2 IgG diluted in milk–PBS-T. The plate was then washed as before, and wells were incubated with various test MAbs (50 μg/ml) in milk–PBS-T containing 50 μg/ml CHL2. After 2 h, the plate was washed and incubated with HRP-conjugated goat anti-mouse Ab (in 5% milk) for 30 min. The plate was then washed and rinsed with 20 mM sodium citrate (pH 4.5). Finally, 100 μl peroxidase substrate (ABTS; Moss, Inc.) was added to the plate, and the absorbance was read at 405 nm. All steps were performed at room temperature.

Optical biosensor analysis. Experiments were carried out on a BIAcore X optical biosensor (BIAcore AB) at 25°C as previously described (1, 22).

(i) Binding properties of IgG to gH2t/gL2 protein. To test the binding properties of our IgGs, an anti-His MAb (QIAGEN, Inc.) was covalently coupled to the BIAcore chip. Next, 250 resonance units of purified gH2t/gL2 was captured by the antibody via its C-terminal His tag. Purified IgGs (20 μg/ml) were then injected, and association was followed for 3 min at room temperature.

(ii) IgG blocking. Blocking studies were performed as previously described (22). For this assay, a primary antibody was allowed to bind for 3 min to the captured gH2t/gL2 protein. A second antibody was then injected, and its association was followed for 3 min.

HSV-2 plaque reduction assay. Monolayers of Vero cells were infected with 50 PFU of HSV-2. At 1 h postinfection, extracellular virus was acid inactivated, and cells were overlaid with DMEM, 5% FBS, and 0.5% carboxymethyl cellulose containing various concentrations of the desired MAb and incubated for 3 days. Monolayers were fixed with 5% formaldehyde-PBS, and plaques were visualized by a black plaque assay (37). Plaques were scored by scanning the plates (HP Scanjet 5500c scanner) and measuring the average number of pixels per plaque per sample.

Selection of mar virus. HSV-2 (strain 333) was added to confluent Vero cell monolayers in 6-cm tissue culture dishes (approximately 500 PFU/plate). After 1 h at 37°C, the virus inoculum was removed, and the plates were overlaid with 5 ml DMEM, 5% heat-inactivated FBS, 1× penicillin-streptomycin (Pen-Strep), 0.5% carboxymethyl cellulose, and 200 μg/ml CHL2 IgG. Plates were incubated at 37°C for 3 to 4 days. Large plaques were picked and transferred to tubes containing DMEM, 5% fetal calf serum, and 1× Pen-Strep. A portion of the medium was transferred to confluent Vero cell monolayers and incubated at 37°C until the cytopathic effect was extensive. Cells were then subjected to three cycles of freezing (−80°C) and thawing (37°C). Virus stocks were serially diluted and added to cells in the presence and absence of 200 μg/ml CHL2. Three rounds of large-plaque selection were carried out. The final purified stock of CHL2 monoclonal antibody-resistant (mar) virus exhibited plaques of similar sizes when added to cells in the presence or absence of CHL2.

Virus neutralization assay. Serial dilutions of MAb were mixed with HSV-2, and the mixture was incubated at 37°C for 1 h. Monolayers of Vero cells grown in 24-well plates were then incubated with the MAb-virus mixture for 1 h at 37°C, after which the remaining extracellular virus was acid inactivated with a solution of 40 mM sodium citrate (pH 3.0), 140 mM NaCl, and 20 mM KCl. Cells were overlaid with DMEM containing 1% carboxymethyl cellulose and 5% FBS and

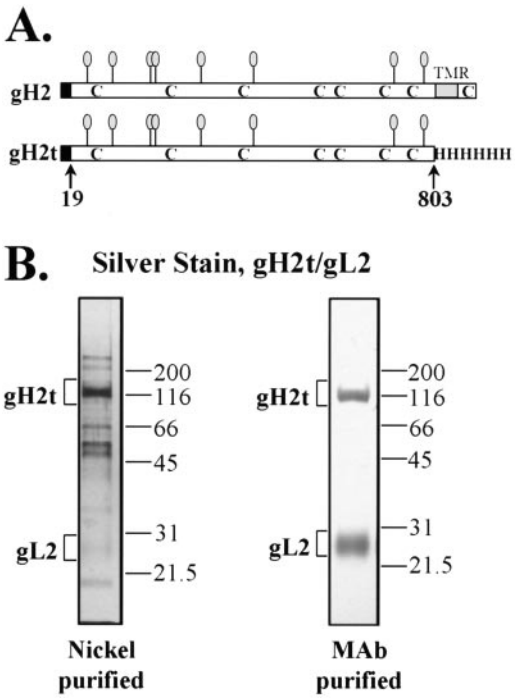

FIG. 1. (A) A truncated form of gH2 (gH2t) in complex with gL2 was used as the immunogen to generate CHL MAbs. gH2 was truncated just prior to the transmembrane region (TMR). The signal sequence (denoted by a black box), cysteines (C), and N-linked glycosylation sites (lollipop structures) are also shown. For purification purposes, a six-His tag was affixed to the gH2t C terminus. (B) Visualization of purified gH2t/gL2 by silver staining. Proteins purified by nickel-affinity chromatography are shown in the left panel, while proteins purified by affinity chromatography using the MAb CHL2 are shown in the right panel. Note that the latter method led to more highly purified products. Size markers (kDa) are indicated to the right of each panel.

incubated for an additional 2 days. Plaques were scored after cells were fixed with 5% formaldehyde-PBS and stained with crystal violet or by black plaque assay.

Cell-cell fusion assay. Plasmids pCAGGS/MCS, pLUC, and pT7-pol were gifts of P. G. Spear (31, 33). Plasmids pTC510 (gH2 wild type [WT]), pTC579 (gL2 WT), pTC580 (gB2 WT), and pTC578 (gD2 WT) were previously described (5). The luciferase reporter gene activation assay (31, 33) was performed in a 96-well format to quantitate cell-cell fusion as described by Cairns et al. (5).

RESULTS

Production of soluble gH2t/gL2. We constructed a baculovirus that carried a soluble form of gH2 (gH2t) that was truncated just prior to the transmembrane domain, at amino acid 803 (Fig. 1A). A histidine tag was engineered at the C terminus of the gH ectodomain to facilitate purification. Full-length gL2 was also cloned into a baculovirus. When cells were coinfected with these two viruses, gH2t/gL2 was abundantly expressed, but most of the complex was trapped in the cells, and very little was secreted. As an alternative approach, we used a mammalian expression system to generate the soluble secreted protein complex. Human 293T cells were transiently transfected with plasmids expressing truncated gH2 and wild-type gL2. Initially, the complex was captured from the culture supernatant via the gH2t His tag, using Ni-nitrilotriacetic acid resin and elution with imidazole (Fig. 1B). This gH2t/gL2 complex was used as the immunogen in our first round of mouse immunizations. Subsequent hybridoma selection yielded 14 MAbs (CHL2 and -4 to -16), and one of these, CHL2, was used as an immunosorbent to purify a second batch of gH2t/gL2 (Fig. 1B). This protein was used as an immunogen and yielded another 17 MAbs (CHL17-43).

Hybridoma selection and anti-gH/gL antibody purification. Mice were subcutaneously inoculated with purified gH2t/gL2. Thirty-one hybridoma cell lines, selected by ELISA reactivity to gH2t/gL2, were established after a minimum of two rounds of clonal selection. IgGs were purified from murine ascitic fluid and were designated CHL2, -4 to -18, -25, -26, -28 to -32, -34 to -39, -41, and -43. None of the MAbs reacted with unrelated proteins that contained a His tag, indicating that they were specifically directed against the recombinant form of gH/gL. A summary of the MAb properties is presented in Table 1.

Purified IgGs were screened for the ability to immunoprecipitate authentic gH/gL from HSV-2-infected cell lysates. Immunoprecipitation of the complex was indicated by the appearance of gH2 in the Western blot shown in Fig. 2A; gL2 was observed but was partially obscured by the IgG heavy chain (data not shown). All of the MAbs except CHL34 immunoprecipitated the complex, suggesting that the epitope for CHL34 was hidden in the native molecule.

The MAbs were next used to probe Western blots containing denatured, purified HSV-1 or HSV-2 gHt/gL. This experiment identified MAbs that recognized linear epitopes of gH or gL. The PAbs R176 (gH2/gL2) and R137 (gH1/gL1) were used to identify gH and gL bands on the blot. All of the MAbs that were generated from mice immunized with immunoaffinity-purified gH2t/gL2 (CHL17-43) recognized denatured gH2/gL2 (Fig. 2B). CHL18, -26, -28, -34, and -39 (boxed in the figure) detected gL2, while the remaining MAbs recognized gH2. In contrast, none of the MAbs that were generated in the first fusion that used nickel-purified gH2t/gL2 as the immunogen (CHL2 and -4 to -16) bound to the denatured virion protein (data not shown). However, these MAbs did recognize gH2/gL2 by immunoprecipitation (Fig. 2A) and ELISA and also worked in immunofluorescence assays of paraformaldehyde-fixed HSV-2 but not HSV-1 (data not shown). These data suggest that MAbs CHL2 and -4 to -16 recognize type-specific, conformation-dependent epitopes (Table 1).

All previously identified gH/gL MAbs are type 1 specific (3, 32, 35). Here we looked for possible type-common MAbs by Western blot analysis of purified HSV-1. Five MAbs cross-reacted with gH1 (CHL27, -29, -30, -31, and -36), and two cross-reacted with gL1 (CHL28 and -34) (Fig. 2C).

Mapping of linear epitopes. A set of overlapping, synthetic peptides was used to finely map the linear gH and gL epitopes recognized by the MAbs. Each peptide contained 20 residues of gH or gL, with the first 11 residues repeating those found in the peptide immediately preceding it in the primary sequence. Each peptide was biotinylated at the N terminus to facilitate binding to streptavidin-coated ELISA plates. Those MAbs designated as having conformation-dependent epitopes (CHL2 and -4 to -16) (Table 1) failed to bind gH2 or gL2 peptides, as expected (data not shown). Mapping of the CHL2 epitope will be described in a later section.

(i) Mapping of gL epitopes using peptide scanning. All five MAbs to gL2 recognized linear epitopes and were mapped by

TABLE 1. Properties of gH/gL MAbs

Group	MAb	Western blot result	Competes with[a]	IP result	Neutralization	Inhibition of spread	Inhibition of fusion	Maps to indicated residues
I	CHL17	gH2		+	+	+	+	19–38
I	CHL32	gH2	CHL17	+	+	−	+	19–38
II	CHL37	gH2		+	−	−	−	28–47
III	CHL25	gH2		+	−	−	−	73–92
IV	CHL41	gH2		+	−	−	−	136–146
Va	CHL31	gH1, 2	CHL35	+	−	−	−	145–155; 676–686
Va	CHL35	gH1, 2	CHL31	+	−	−	−	145–155
Vb	CHL36	gH1, 2		+	−	−	−	145–155
VI	CHL38	gH1, 2		+	−	−	−	352–371
VII	CHL43	gH2		+	−	−	−	532–542
VIII	CHL29	gH1, 2	CHL30	+	−	−	−	676–686
VIII	CHL30	gH1, 2	CHL29	+	−	−	−	145–155; 676–686
IX[c]	CHL2	None	CHL4-16	+	−	+	−	mar 116
IX[c]	CHL4-16	None	CHL2	+	−	+	ND[b]	ND[b]
A	CHL28	gL1, 2		+	−	−	−	146–165; 205–219
A	CHL34	gL1, 2	CHL28	−	−	−	−	146–165; 205–219
B	CHL18	gL2	CHL26	+	−	+	−	205–210
B	CHL26	gL2	CHL18	+	−	−	−	182–219
C	CHL39	gL2		+	−	+	−	191–201

[a] Competition analysis was done by ELISA for CHL2 and -4 to -16 and by biosensor analysis for all other MAbs.
[b] ND, not done.
[c] MAbs in this group were positive by an immunofluorescence assay.

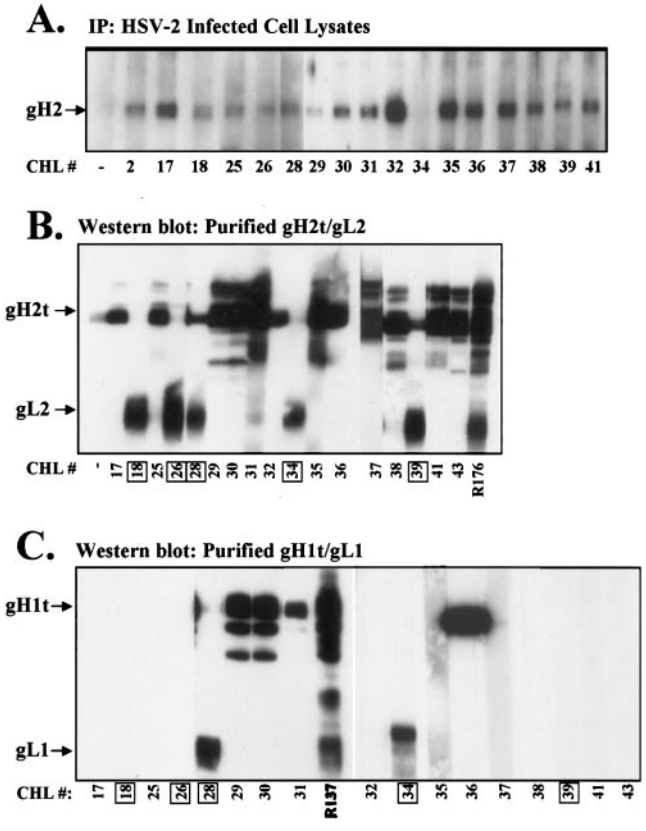

FIG. 2. Most CHL MAbs recognize gH/gL complexes from HSV-2-infected cells and purified gHt/gL protein. (A) gH/gL present in lysates of HSV-2-infected cells was immunoprecipitated with each one of the anti-gH/gL MAbs, separated by SDS-polyacrylamide gel electrophoresis, and analyzed by Western blotting. Blots were probed with the PAb R176 to detect gH2. Purified, denatured gH2t/gL2 (B) or gH1t/gL1 (C) was separated by SDS-polyacrylamide gel electrophoresis, and separate nitrocellulose strips were probed with each of the MAbs. MAbs that recognized gL are boxed. An anti-Myc MAb (−) was used as a negative control.

ELISA using the 22 overlapping synthetic peptides diagrammed in Fig. 3A. The background signal was routinely quite low (Fig. 3B). CHL39 bound to overlapping peptides, 19 and 20, that spanned amino acids 182 to 210. We consider the CHL39 epitope to be within the overlap, and therefore it is defined as residues 191 to 201 (Table 1).

CHL26 and CHL18 each bound three overlapping peptides. In the case of CHL26, these were peptides 19 to 21, spanning residues 182 to 219. Only two amino acids overlap. Therefore, we were unable to confidently narrow the binding region any further for this MAb, although we think the epitope must include residues 200 and 201. CHL18 bound equally well to peptides 20 to 22, spanning residues 191 to 224. In this case, the overlap was within amino acids 205 to 210.

An unexpected pattern of peptide reactivity was observed for CHL28 and CHL34. In these two cases, the MAbs bound to two overlapping peptides, 21 and 22 (residues 200 to 224, with the overlap between residues 205 and 219) but also bound to the upstream peptide 15 (residues 146 to 165). Because CHL28 and -34 bound two separate regions in the linear sequence of gL2, we were concerned that the cell lines might not be clonal, i.e., there might be two populations of cells secreting Abs that recognized one set of peptides or the other. However, RT-PCR showed that the cloned hybridoma cells for these two MAbs each produced only one light chain (see Materials and Methods), demonstrating that they are indeed clonal. It is possible that these two regions (residues 146 to 165 and 205 to 219) are located close together in the folded structure and form a shared epitope. Alternatively, the MAbs could cross-react with amino acids in common between the two regions, such as the two sets of double arginines (RR and GRR) shown in Table 2.

(ii) Biosensor studies to assess the ability of anti-gL MAbs to block binding of each other to gH2t/gL2. In ELISAs, binding of protein to the plate surface is thought to be random, with the result that all of the epitopes are statistically represented.

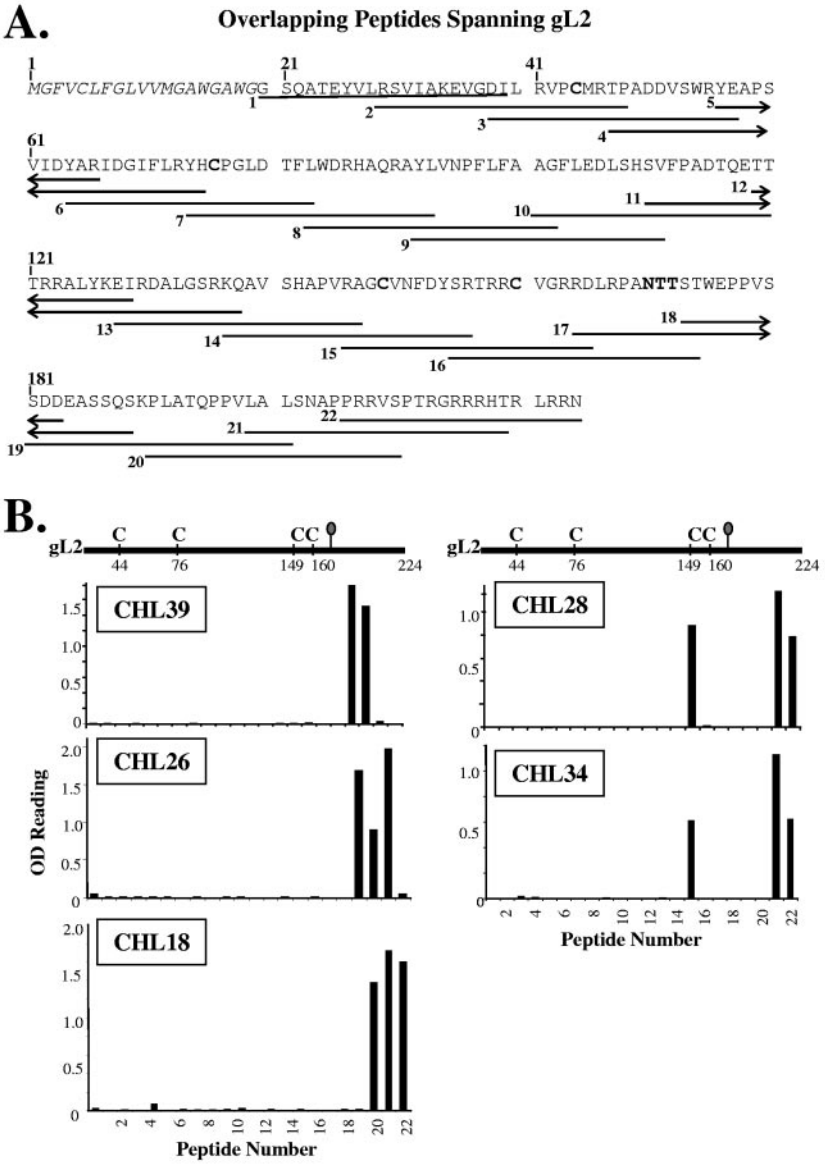

FIG. 3. (A) Schematic representation of gL2 peptides. Each peptide is depicted by a black line under its corresponding amino acid sequence. The peptide number is shown to the left of each line. No peptides were made to the signal sequence (italicized). (B) Epitope mapping by peptide-ELISA. Each peptide was solubilized, added to a well of a 96-well streptavidin-coated plate, and allowed to bind at room temperature for 1 h. The wells were then blocked and probed with MAb. Bound IgG was visualized with goat anti-mouse–HRP. A linear representation of gL2, aligned with the peptide numbers on the *x* axis of the graph, is provided as a visual reference at the top. Cysteine residues are depicted (C), and the amino acid number of each is provided. N-linked glycosylation sites are denoted by lollipop structures.

However, absorption of the protein directly to the plate may alter its native conformation. In the biosensor assay, an anti-His antibody was covalently coupled to the chip and gH2t/gL2 was captured by its His tag, thus presenting the complex in its native state. Reciprocal blocking assays were carried out with each MAb to assess their abilities to block each other (Fig. 4 and Table 1). The rationale is that if the second MAb fails to bind to gH2t/gL2, its epitope overlaps that recognized by the primary MAb. If the second MAb binds, then its epitope is independent of the epitope bound by the first MAb (1, 22). Data from one such experiment are shown in Fig. 4A. First, the primary antibody CHL34 was bound to the captured gH2t/gL2, with the signal leveling off at approximately 90 resonance units. The secondary (test) antibody, either CHL39 or CHL28, was then injected, and its binding was monitored. In the case of CHL39, the increase to 220 resonance units indicated that it could bind to gL even when CHL34 was already bound. We interpret this to mean that the two MAbs recognize different gL2 epitopes. However, when this was done with CHL28, no increase in resonance units was detected over that caused by the binding of CHL34. In this case, we conclude that CHL28 and CHL34 recognize overlapping epitopes. Interestingly, in this case, blocking was nonreciprocal, i.e., when CHL28 was bound first, CHL34 was also able to bind (data not shown). We

TABLE 2. Sequence comparison of noncontiguous peptides bound by a single MAb

Group(s)	Protein	MAbs	Residues (amino acid sequence)[a]
A	gL	CHL28, -34	146–165 (VRAGCVNFDYSRTRRCV---GRRD--) 205–219 (----------PPRRVSPTRGRRRHT) ** ***
Va, VIII	gH	CHL30, -31	145–155 (SHNPGASALLR) 676–686 (THTPLPRGIGY) * *

[a] A dash indicates a skip in the linear sequence; an asterisk indicates amino acid identity.

believe this means that the epitopes are overlapping but not identical, although both MAbs bound to the same set of synthetic peptides (Fig. 3B). Nonreciprocal binding may also indicate differences in affinity (1). In contrast, another MAb pair, CHL18 and CHL26, did exhibit reciprocal blocking, suggesting that some residues between residues 205 and 210 are shared (Fig. 4B).

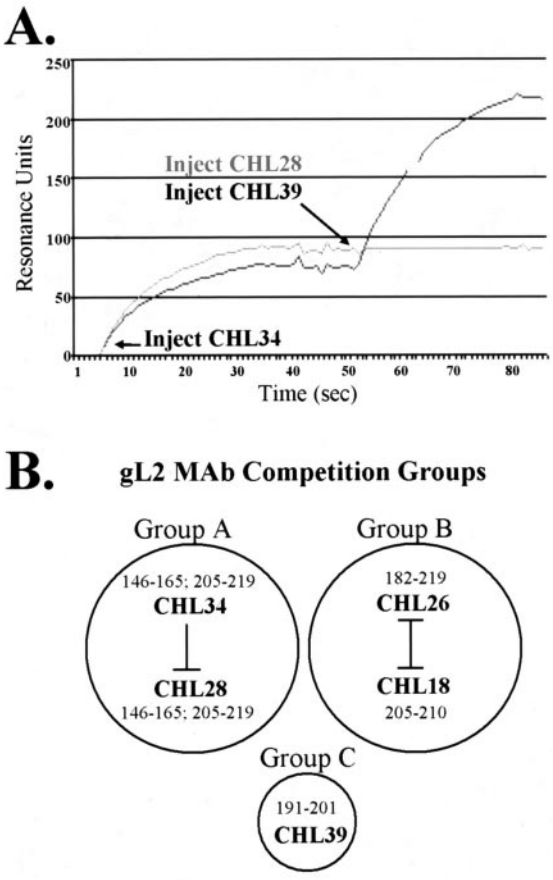

FIG. 4. Biosensor analysis defines three competition groups within gL2. (A) Representative graph showing binding properties of CHL34, -28, and -39. The biosensor chip was coated with gH2t/gL2 (purified by MAb affinity chromatography). CHL34 was bound to gH2t/gL2 first, followed by either CHL28 (competed) or CHL39 (did not compete). (B) Visual depiction of gL2 competition groups. Lines drawn between CHL MAbs within the same circle indicate binding competition (I represents reciprocal competition, while an upside-down T represents nonreciprocal competition). CHL39, which binds the same region of gL2 as CHL26 and -18 (as determined by peptide-ELISA), nevertheless does not compete with either of these MAbs for protein binding.

Based on the biosensor data, the anti-gL MAbs were placed into three groups (Fig. 4B). First, MAbs CHL28 and CHL34 are in group A since CHL34 blocked CHL28 binding. These two MAbs bound to the same peptides in two separate regions of the linear gL2 sequence. CHL18 and CHL26 were assigned to group B. CHL39 did not compete with any other MAbs and was assigned to group C. The fact that this MAb did not compete with other MAbs is intriguing, as it recognized peptide 19 (which was also bound by CHL26) and peptide 20 (which was bound by CHL26 and CHL18). Our epitope mapping data for the five gL2 MAbs suggest that the region of gL2 spanning residues 182 to 224 is highly immunogenic and contains multiple epitopes.

(iii) Mapping of gH2 epitopes using peptide scanning. A set of 88 peptides was used to map gH-specific MAbs, using the same approach as that used for the gL MAbs (Fig. 3). We defined eight distinct linear epitopes (within antigenic sites designated I to VIII) that were spaced across the gH2 ectodomain (Fig. 5A and Table 1). The results of three representative ELISAs are shown in Fig. 5B. CHL25 reacted with one peptide that spanned amino acids 73 to 92. CHL29 reacted with two overlapping peptides, and its epitope was narrowed to amino acids 676 to 686. A total of six epitopes were located in the N-terminal half of gH2, including residues 19 to 38 (site I), 28 to 47 (site II), 73 to 92 (site III), 136 to 146 (site IV), 145 to 155 (site V), and 352 to 371 (site VI). Several other MAbs mapped to amino acids in the C-terminal half, within residues 532 to 542 (site VII) and 676 to 686 (site VIII). As seen with the gL2 MAbs CHL28 and CHL34 (Fig. 3B), two gH2 MAbs, CHL30 and CHL31, bound noncontiguous peptides corresponding to sites V and VIII (Fig. 5B). Both were determined to be clonal by RT-PCR (data not shown; see Materials and Methods).

(iv) Biosensor studies to assess the ability of anti-gH MAbs to block binding of each other to gH2t/gL2. Prior to blocking assays, each gH2 MAb was tested for its ability to bind gH2t/gL2 by a biosensor assay. MAbs CHL2 and -4 to -16 bound poorly to the captured gH/gL complex; however, MAbs CHL17-43 bound sufficiently well to gH/gL that we were able to test them for competition of binding (data not shown). As with the gL2 MAbs, reciprocal blocking assays were carried out with each of these MAbs (Table 1; data not shown). Eight groups of MAb reactivity were observed, matching those defined by peptide analysis, with a few exceptions which hinted at the complexity of some of the epitopes. In one case, CHL35 and -36 recognized peptides that placed their epitopes within residues 145 to 155 (site V according to peptide analysis) (Fig. 5A). However, these two MAbs failed to block each other by

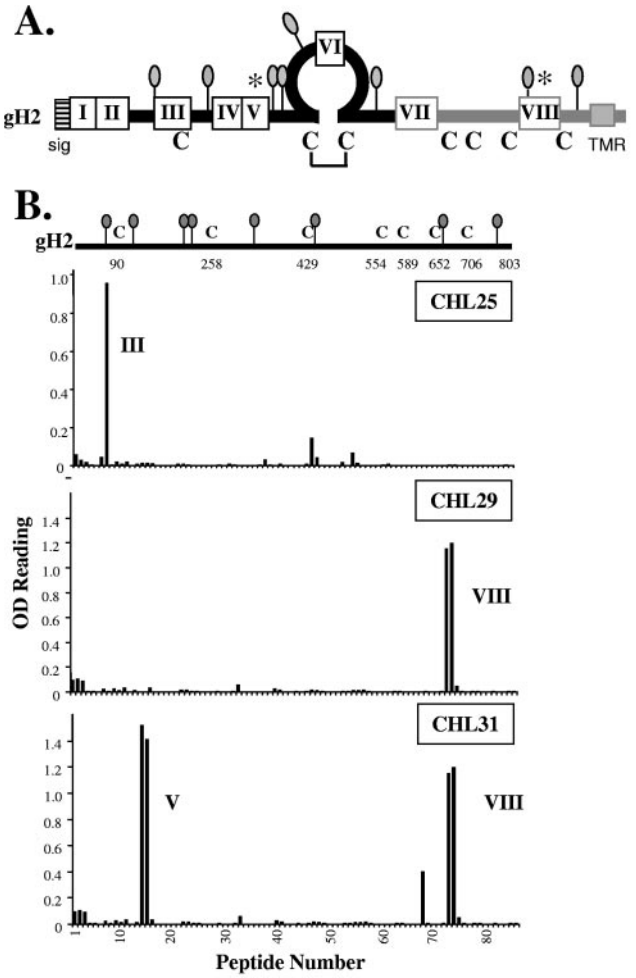

FIG. 5. gH2 has eight antigenic sites across its ectodomain. (A) Schematic of gH2 highlighting its antigenic regions. The black line represents the gH2 N-terminal domain, and the gray line represents the C-terminal domain. Epitopes I through VIII are outlined with white boxes. The gH signal sequence (sig) is depicted as a striped box, and the transmembrane region (TMR) is shown as a gray box. Cysteines and N-CHO sites are represented as in Fig. 1. The hypothesized C2-C4 disulfide bond is shown as a bracket linking these two cysteines. The asterisks indicate that some anti-gH MAbs bind both of these regions. (B) Epitope mapping by peptide-ELISA was performed as described in the legend to Fig. 3. A linear representation of gH2, aligned with the peptide numbers on the *x* axis of the graph, is provided as a visual reference at the top. Group designations are provided to the right of the bars of the reactive peptides.

biosensor analysis (data not shown). Therefore, they were subdivided into groups Va (CHL35) and Vb (CHL36) (Fig. 6 and Table 1). In a second instance, the group I MAbs CHL17 and -32 displayed nonreciprocal competition, similar to that seen for two gL2 MAbs (Fig. 4B and Table 1). In the last case, MAbs CHL30 and -31 recognized peptides in different regions of gH2 (sites V and VIII) (Fig. 5A and B). On the basis of blocking, they were placed into either group Va (CHL31) or group VIII (CHL30). As expected (given the unique positions of their epitopes), all other MAbs failed to block the binding of any other gH2 MAb.

Thus, a combination of peptide mapping and biosensor analysis allowed us to map the epitopes for 17 MAbs against gH2 and gL2. We defined eight antigenic sites on gH2 and three on gL2. Five of the gH2 sites (I to V) lie within the gL binding region (32), and one (site VIII) encompasses a portion of gH that is important for fusion (14).

Association of biological functions within defined regions of gH/gL. Having mapped many of the MAbs, we wanted to test them for biological activity so that we could relate function to structure. First, we examined the ability of the MAbs to block the fusion of effector cells expressing gH/gL in combination with gB and gD and with target cells expressing the gD receptor HVEM (5, 33). Of all the MAbs tested, only CHL17 and -32 were able to block fusion by >50% the level of the control MAb (Fig. 7A). Several other Abs (CHL2, CHL18, CHL37, and the PAb R176) reduced fusion to approximately 60% that of the control. Both of the MAbs that blocked fusion bound the same region of gH2 (site I; residues 19 to 38). In comparison, the PAb R149, which was generated from immunization with a gH2 peptide encompassing residues 21 to 38, reduced fusion to approximately 55% that of the control.

As a second test of function, the panel of gH2/gL2 MAbs was tested in a virus neutralization assay (Fig. 7B). CHL17 and -32 showed moderate levels of neutralizing activity (roughly 50% that of the control MAb) and were similar to PAb R176 on a microgram- of-IgG basis (Fig. 7C). Interestingly, these two MAbs blocked function in both fusion and virus neutralization assays. None of the other CHL MAbs neutralized the virus.

Finally, the antibodies were tested for the ability to inhibit cell-cell spread of HSV-2 infection. Vero cells were infected at a low multiplicity with HSV-2 and then overlaid with a methylcellulose-DMEM mixture that contained one of the MAbs. After 3 days, the monolayers were scored for plaque number and size (Fig. 8A). All of the MAbs that bound conforma-

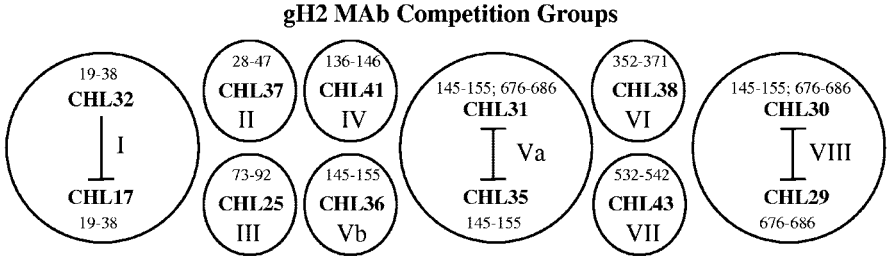

FIG. 6. Biosensor analysis defines competition groups within gH2. Biosensor analysis was performed as described in the legend to Fig. 4. Nine competition groups for the 12 MAbs that recognize linear epitopes are shown.

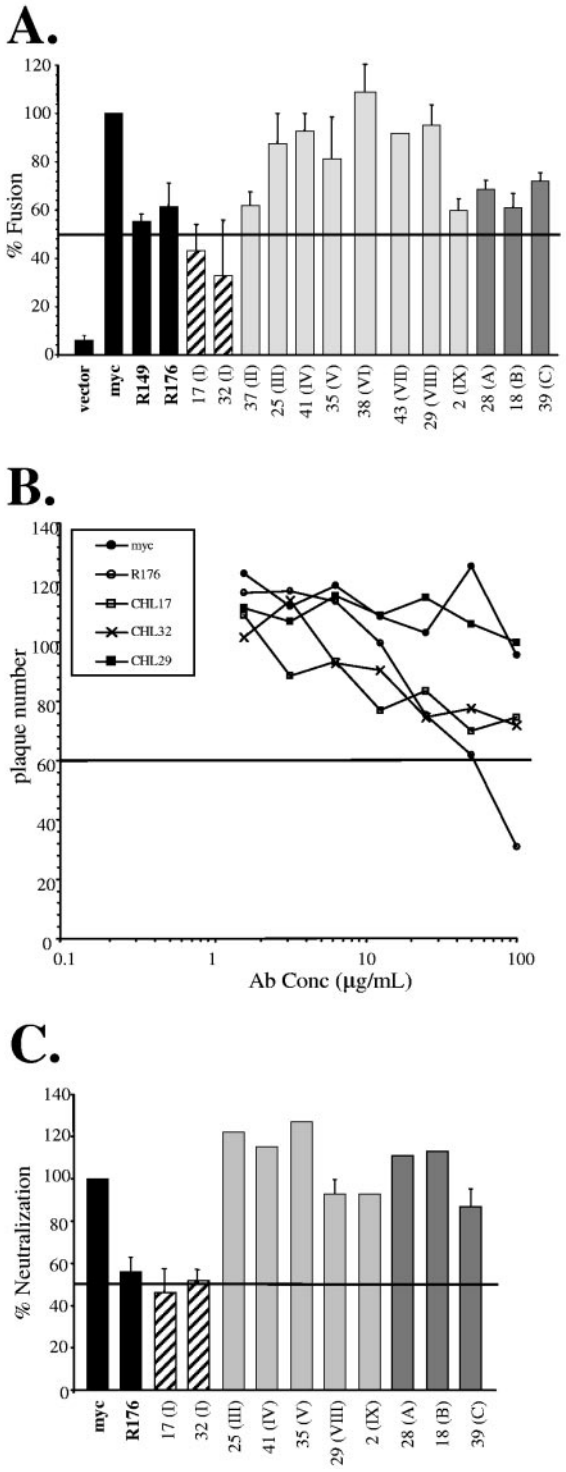

FIG. 7. Certain CHL MAbs affect gH/gL function. (A) MAbs CHL17 and -32 inhibit cell-cell fusion >50% compared to the control Ab (myc). Results were graphed as percentages of WT fusion seen with no Ab (in relative units [RU]), as follows: % control = (RU with experimental Ab)/(RU with control Ab) × 100. The averages of at least three separate experiments are shown (with the exception of CHL43). Those samples that exhibited fusion below 50% that of the control (solid black line) were scored as positive for fusion inhibition. (B) MAbs CHL17 and -32 weakly neutralize HSV-2 on Vero cells. Sequential dilutions of Ab were mixed with HSV-2 and incubated at 37°C for 1 h. Vero cells were then infected with the MAb-virus mixture for 1 h at 37°C, after which the virus was acid inactivated. After 2 days, cells were fixed, stained, and scored for plaque formation. All CHL MAbs and the PAb R176 were tested, with results for CHL17, -32, and -29 shown as a representative experiment. (C) Bar graph depicting percent neutralization at 50 μg/ml IgG. CHL17, -32, -29, and -39 were scored for at least three separate experiments; the remaining MAbs did not neutralize virus, resulting in many plaques that we visualized but did not count. Results were graphed as percentages of the number of plaques with the control Ab (myc), as follows: % control = (number of plaques with experimental Ab)/(number of plaques with control Ab) × 100 (taken at 50 μg/ml IgG). CHL MAbs are indicated in each graph by their numbers, followed by their MAb group numbers in parentheses (Roman numerals).

tion-dependent epitopes (CHL2 and -4 to -16) inhibited cell-cell spread of the virus, as indicated by a 70% reduction in plaque size (represented by CHL2 in Fig. 8B). Two anti-gL MAbs, CHL18 and -39, also reduced plaque size by 70% and 45% that of control plaques, respectively. CHL17, which recognizes an epitope within site I of gH2 (residues 19 to 38), was the only MAb that inhibited both spread and cell-cell fusion and also neutralized virus infection (Table 1). The other MAb in gH2 group I, CHL32, did not inhibit plaque size. The observation that CHL17 and -32 behaved differently in the spread assay fits with the nonreciprocal blocking seen between these MAbs during biosensor analysis. In conclusion, the functional assays highlighted two regions within gH/gL, i.e., site I (residues 19 to 38) on gH and sites B and C (residues 191 to 210) on gL, that may be important for virus entry and spread.

Use of a mar mutant to map CHL2. Since MAbs CHL2 and -4 to -16 all blocked cell-cell spread, we decided to obtain more information about the locations of their discontinuous epitopes by selection of a mar mutant virus. As in the virus spread assay, Vero cells were infected with HSV-2, and after 1 h, the virus inoculum was removed and cells were overlaid with complete growth medium containing carboxymethyl cellulose and CHL2. After 3 days, large plaques were picked, and the virus was used to infect more Vero cells; three rounds of plaque selection in the presence of the MAb CHL2 were carried out. The final plaque-purified virus (designated marH-CHL2) produced large plaques in the presence or absence of CHL2 (Fig. 9). Sequencing of the gH and gL open reading frames from marH-CHL2 revealed a G-to-D change at residue 116 of gH2. There were no changes in the gL coding sequence. Unlike WT HSV-2, marH-CHL2 was not immunoprecipitated by CHL2 IgG (data not shown), indicating that glycine 116 is a critical part of the CHL2 epitope, thus mapping it at least in part to the N-terminal half of gH2.

DISCUSSION

Although it is clear that the gH/gL complexes of HSV-1 and HSV-2 play an essential role in virus entry and cell-cell spread of HSV (36), very few immunologic reagents were previously available to either identify important functional regions or gain information about structural features of these proteins. It is noteworthy that one of these MAbs, LP11 (3), is directed to an epitope in the gH1/gL1 complex and has significant virus neutralizing activity. LP11 has been used as the "gold standard"

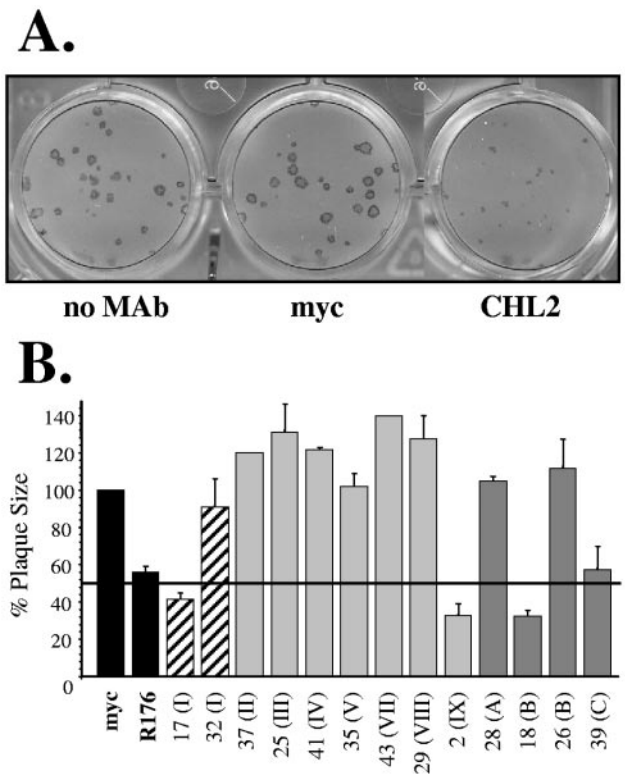

FIG. 8. Several CHL MAbs inhibit cell-cell spread of HSV-2. Vero cells were infected with HSV-2 for 1 h, overlaid with 100 μg/ml of the desired MAb, and then incubated for 3 days. Results of a representative experiment are shown in panel A. (B) Plates were scanned with an HP Scanjet 5500c scanner, and plaques were scored for size by measuring the average number of pixels per plaque. Those samples that generated plaques that had at least a 50% reduction in plaque size (solid black line) were scored as positive for inhibition of cell-cell spread. Results were graphed as percentages of the number of pixels/plaque seen with no Ab, as follows: % control = (pixels with experimental Ab)/(pixels with no Ab) × 100. The averages of at least two separate experiments are shown. CHL MAbs are indicated in the graph by their numbers, followed by their MAb group numbers in parentheses (Roman numerals).

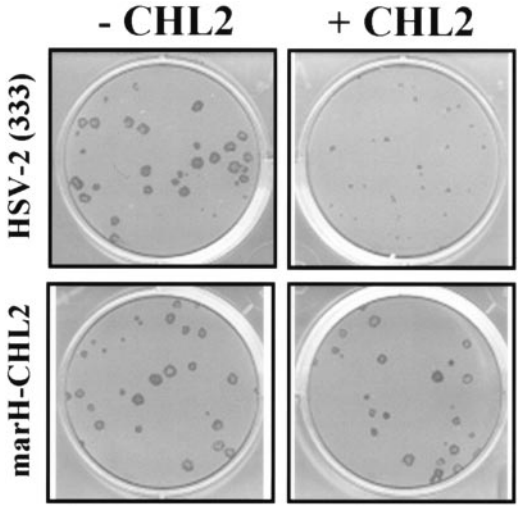

FIG. 9. Generation of marH-CHL2 virus. Approximately 500 PFU/plate of HSV-2 was added to confluent Vero cell monolayers. After 1 h, the virus was removed, and an overlay containing 200 μg/ml CHL2 IgG was placed on the cells. Plates were incubated at 37°C for 3 to 4 days, after which large plaques were picked and replated for three rounds of plaque selection. The final purified stock of CHL2 mar virus exhibited plaques of similar sizes in either the presence or absence of CHL2 IgG (200 μg/ml).

for the assessment of gH1/gL1 integrity as well as for mutagenesis and biochemical experiments (3–5, 12, 14, 18, 19, 32). However, until this report, most, if not all, of the existing MAbs (including LP11) were type 1 specific. Thus, the field has been hampered by a general shortage of reagents and, in particular, the paucity of MAbs to gH2 or gL2.

The goal of the studies presented here was to create and study a new panel of MAbs, using gH2/gL2 as the immunogen. After two rounds of hybridoma selection and purification, we amassed a total of 31 MAbs, including some that recognized only gH or gL and some that recognized the complex of the two proteins. We were fortunate to find eight cross-reactive MAbs, six of which recognized both gH1 and gH2 and two of which recognized gL1 and gL2. The new panel of MAbs enabled us to carry out the first detailed antigenic analysis of structural and functional regions of gH2 and gL2. Flow charts (Fig. 10 and 11) summarize the properties of the gH and gL MAb groups defined here and also include properties of the known MAbs to gH1 and gL1. Our studies defined eight groups of MAbs specific to gH2 (designated groups I to VIII) and one group (IX) of MAbs specific to the gH2/gL2 complex. Six other groups of previously described MAbs to gH1 were designated groups X to XV (3, 18, 32, 35). We also defined three groups of MAbs to gL2 (designated groups A to C). A fourth group (group D) consists of previously described MAbs that are gL1 specific (9, 30, 32). Thus, according to our scheme, there are now a total of 15 groups of MAbs that define antigenic sites on gH1 and/or gH2 and 4 groups of MAbs that define antigenic sites on gL1 and/or gL2.

Antibodies predict aspects of gH/gL structure. Immunoprecipitation studies using polyclonal antibodies to peptides mimicking the N terminus of gL1 showed that these residues are inaccessible to antibodies in the gH/gL complex (20, 32). As found for gL1 (4, 30, 32), none of our gL2 MAbs recognized amino acids prior to residue 145, which encompasses the proximal two-thirds of the protein. This observation is additional evidence that the N-terminal 145 residues of gL are buried within the N terminus of gH and that residues 147 to 224 are exposed.

It is important that none of the gL MAbs inhibited the binding of any gH MAbs, and vice versa (Table 1; data not shown). Therefore, we are unable to predict precisely which regions of the two proteins might be close together in the folded complex. Interestingly, four MAbs recognized multiple, noncontiguous peptides of gH2 or gL2, a phenomenon that has been seen with several MAbs for other proteins (1; F. Bender, personal communication). In the present study, MAbs CHL30 and CHL31 bound the same set of peptides (spanning positions 145 to 155 and 676 to 686). Biosensor analysis showed that CHL30 and -31 bind to different epitopes, as they do not block each other. However, each of these MAbs was blocked by different MAbs at opposite ends of gH (Fig. 6 and Table 1).

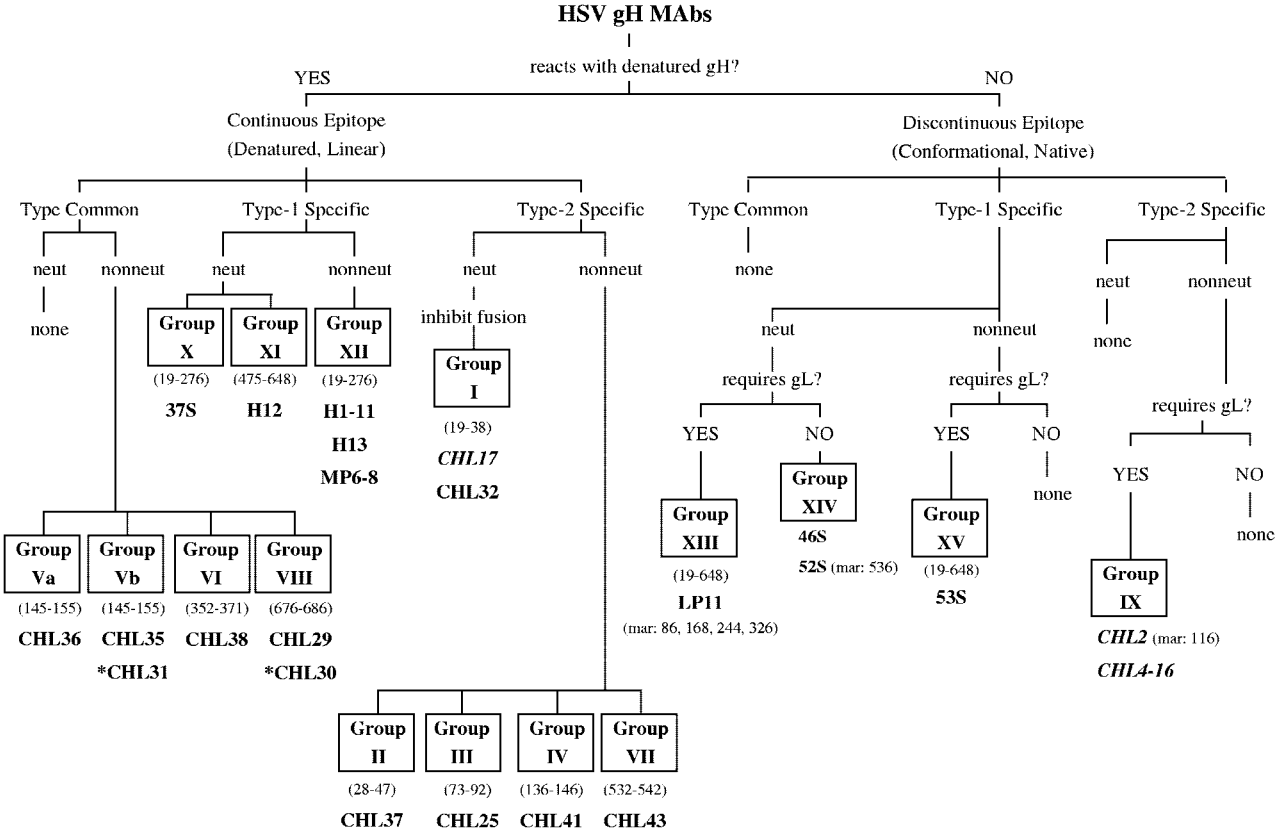

FIG. 10. Diagram of HSV gH MAbs published to date (3, 14, 18, 19, 30, 32, 35). MAbs written in italics inhibit cell-cell spread. neut, neutralizing MAb; nonneut, nonneutralizing MAb; *, CHL30 and -31 bind residues 145 to 155 and 676 to 686 but are grouped according to biosensor analysis data.

How the properties of these MAbs relate to the gH structure is not clear, but we speculate that residues 145 to 155 and 676 to 686 may be near each other in the folded structure. It is unlikely that CHL30 and -31 recognize residues common to both peptides (residues 145 to 155 and 676 to 686), since only two amino acids are common to these sequences and they are not contiguous (Table 2).

In contrast to the unique situation for CHL30 and -31, two gL MAbs, CHL28 and -34, each recognized two noncontiguous peptides, and the two MAbs appear to be related to each other. CHL34 blocked the binding of CHL28 to gL2, although the reverse was not true. In this case, it is at least possible that the data can be explained by the presence of a repetitive stretch of amino acids in the two parts of the protein. An examination of the primary protein sequence corresponding to the noncontiguous peptides revealed two short stretches of residues (RR and GRR) common to both sets of peptides (Table 2). However, it is also possible that the epitopes for these two MAbs consist of residues in two regions of gL, both of which have enough affinity for the MAbs that they bind to each peptide individually. If this is the case, then residues 146 to 165 of gL would be spatially near the C-terminal residues 205 to 219. The fact that CHL28 and CHL34 are type common may offer an additional clue about their epitopes. Residues 205 to 219 are only 47% identical in gL1 and gL2 (Table 3), but residues 146 to 165 are 90% identical. We hypothesize that the epitopes for these MAbs are mostly contained within the latter stretch of amino acids.

MAbs identify functions of gH and gL and define functional regions. Fuller and Lee (13) showed that HSV-1 binds to cells and forms a fusion bridge with the plasma membrane in the presence of the anti-gH neutralizing antibody LP11 (3). However, the fusion bridge is unable to expand, implying that LP11 prevents this final step of virus-cell fusion. MAbs to gH also inhibit virus-cell fusion of human herpesvirus 6 (23), Epstein-Barr virus (26), and Kaposi's sarcoma herpesvirus (28). Certain anti-gL Abs inhibit plaque formation by a syncytial strain of HSV without affecting viral infectivity (30). These MAbs provide insight into potential differences in gH and gL function. MAbs that inhibit one glycoprotein function but not another (e.g., fusion but not entry) are also helpful in investigating differences between virus entry, cell-cell fusion, and virus spread.

In this study, the following three different types of MAbs affected gH2/gL2 function: (i) MAbs that bound conformation-dependent epitopes of the gH/gL complex (CHL2 and -4 to -16), (ii) MAbs that bound linear epitopes of gH2 within residues 19 to 28 (CHL17 and -32), and (iii) MAbs that bound linear epitopes within residues 182 to 224 of gL2 (CHL18 and -39). These MAbs highlight regions that we regard as targets for further analysis. It is noteworthy that residues 19 to 28 of gH have not been selected by computer searches for functional motifs such as fusion peptides or coiled-coil domains. Using

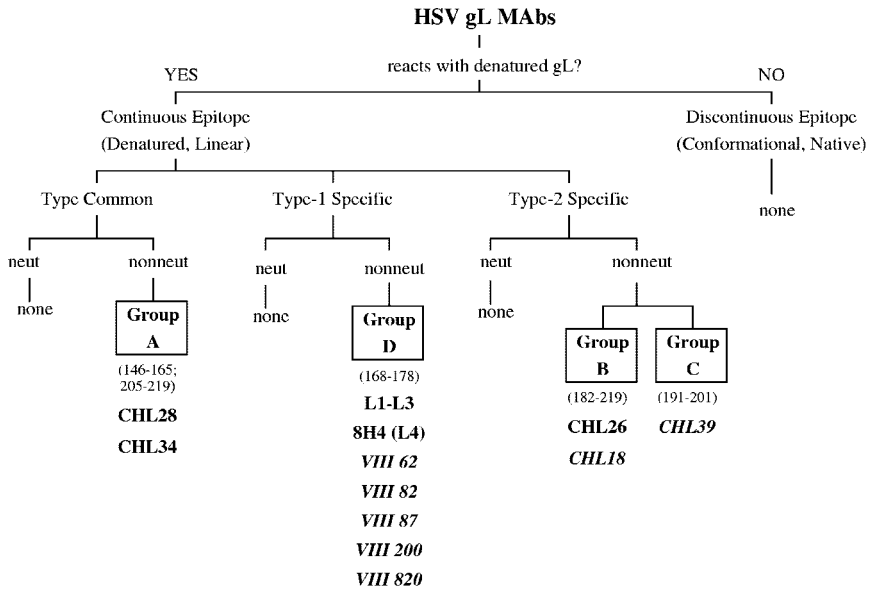

FIG. 11. Diagram of HSV gL MAbs published to date (9, 30, 32). MAbs written in italics inhibit cell-cell spread. neut, neutralizing MAb; nonneut, nonneutralizing MAb.

computer predictions, Gianni et al. (16, 17) identified two other regions of gH1 (residues 377 to 397 and 445 to 472) that might contain fusion peptide motifs and found that synthetic peptides mimicking these residues blocked virus entry. In addition, they created a synthetic peptide corresponding to residues 381 to 420 that fused liposomes in vitro. A potential coiled-coil domain was located within residues 445 to 472 of human cytomegalovirus gH (25). For HSV-2 gH, this region is not predicted to form a coiled coil and is only marginally predicted to form a heptad repeat.

TABLE 3. Sequence comparison of type 1 versus type 2 protein regions

Group	Type	Residues	Region (amino acid sequence)[a]	% Identity
A	Common	146–165	gL1 (KAGCVNFDYSRTRRCVGRQD) gL2 (RAGCVNFDYSRTRRCVGRRD) ********** *	90
B,C	Specific	182–219	gL1 (DDEAGLQPKPLTTPPPIIATSDPTPRRDAATKSRRRRP) gL2 (DDEASSQSKPLATQPPVLALSNAPPRRVSPTRGRRRHT) **** * *** * ** * * *** * ***	53
I	Specific	19–38	gH1 (QVHDWTEQTEPWFLDGLGMDR) gH2 (HDTYWTEQIEPWFLHGLGLAR) **** ***** *** *	62
II	Specific	28–47	gH1 (EPWFLDGLGMDRMYWRDTNTG) gH2 (EPWFLHGLGLARTYWRDTNTG) ***** *** * ********	81
III	Specific	73–92	gH1 (LNLTTASLPLLRWYEERFCF) gH2 (LNLTTASVPMLRWYAERFCF) ******* * **** *****	85
IV	Specific	136–146	gH1 (PPAVAPLKGLL) gH2 (PAEVTQLKGLS) * * ****	54
Va,b	Common	145–155	gH1 (LLHNPTASVLL) gH2 (LSHNPGASALL) * *** ** **	73
VI	Common	352–371	gH1 (YAQFLSRAYAEFFSGDAGAE) gH2 (YAQYMSRAYAEFLGEDPGSG) *** ******* * *	60
VII	Specific	532–542	gH1 (AGVPSAVQRER) gH2 (AGAPSAEQRER) ** *** ****	82
VIII	Common	676–686	gH1 (THSPLPRGIGY) gH2 (THTPLPRGIGY) ** ********	91

[a] Asterisks indicate identical amino acids between types 1 and 2.

For gL, our findings point to the gL2 C terminus as being important for function. MAbs targeted to this region inhibited cell-cell fusion to 40% of WT levels. These MAbs also effectively disrupted cell-cell virus spread, although they were unable to inhibit virus entry (Fig. 11). Both virus entry and spread involve membrane fusion, but our data emphasize that the two processes are distinct and involve different regions of the gH/gL complex.

In conclusion, we have generated a new set of reagents for studying HSV gH/gL. The 31 MAbs described here recognize eight regions spread across the gH ectodomain and three regions clustered near the C terminus of gL. In addition, we isolated MAbs that recognize at least one conformation-dependent epitope of the gH2/gL2 complex. A mar mutant indicated that at least one of the MAbs (CHL2) recognizes amino acids of gH2. We integrated this new panel with those MAbs to gH1 and gL1 that have already been described to provide a comprehensive antigenic map of these proteins. Neutralization and cell-cell fusion and spread assays have highlighted two specific regions, one at the N terminus of gH and the other at the C terminus of gL, that are important for gH2/gL2 function. We are currently examining these regions more closely to gain further insights about the role of gH/gL in HSV entry and spread.

ACKNOWLEDGMENTS

Funding for this project was obtained through NIH grant NS36731 to R.J.E. from the National Institute of Neurologic Disorders and Stroke and grants AI-18289 and AI-056045 to G.H.C. and R.J.E., respectively, from the National Institute of Allergy and Infectious Diseases.

We are grateful to P. G. Spear for providing reagents. We also thank L. Aldaz-Carroll, H. Lou, C. Krummenacher, and K. Stiles for technical support.

REFERENCES

1. **Aldaz-Carroll, L., J. Whitbeck, M. Ponce-de-Leon, H. Lou, L. Hirao, S. N. Isaacs, B. Moss, R. J. Eisenberg, and G. C. Cohen.** 2005. Epitope mapping studies define two major neutralization sites on the vaccinia virus EEV glycoprotein B5R. J. Virol. **79:**6260–6271.
2. **Anderson, R. A., D. X. Liu, and U. A. Gompels.** 1996. Definition of a human herpesvirus-6 betaherpesvirus-specific domain in glycoprotein gH that governs interaction with glycoprotein gL: substitution of human cytomegalovirus glycoproteins permits group-specific complex formation. Virology **217:**517–526.
3. **Buckmaster, E. A., U. Gompels, and A. Minson.** 1984. Characterisation and physical mapping of an HSV-1 glycoprotein of approximately 115 × 10(3) molecular weight. Virology **139:**408–413.
4. **Cairns, T., R. S. B. Milne, M. P. d. Leon, D. K. Tobin, G. H. Cohen, and R. J. Eisenberg.** 2003. Structure-function analysis of herpes simplex virus (HSV-1) gD and gH/gL: clues from gD/gH chimeras. J. Virol. **77:**6731–6742.
5. **Cairns, T. M., D. J. Landsburg, J. C. Whitbeck, R. J. Eisenberg, and G. H. Cohen.** 2005. Contribution of cysteine residues to the structure and function of herpes simplex virus gH/gL. Virology **332:**550–562.
6. **Carfi, A., S. H. Willis, J. C. Whitbeck, C. Krummenacher, G. H. Cohen, R. J. Eisenberg, and D. C. Wiley.** 2001. Herpes simplex virus glycoprotein D bound to the human receptor HveA. Mol. Cell **8:**169–179.
7. **Chiang, H.-Y., G. H. Cohen, and R. J. Eisenberg.** 1994. Identification of functional regions of herpes simplex virus glycoprotein gD by using linker-insertion mutagenesis. J. Virol. **68:**2529–2543.
8. **Coligan, J. E., A. M. Kruisbeek, D. H. Margulies, E. M. Shevach, and W. Strober (ed.).** 1994. Current protocols in immunology, vol. 1. John Wiley & Sons, Inc., New York, N.Y.
9. **Dubin, G., and H. Jiang.** 1995. Expression of herpes simplex virus type 1 glycoprotein L (gL) in transfected mammalian cells: evidence that gL is not independently anchored to cell membranes. J. Virol. **69:**4564–4568.
10. **Eisenberg, R. J., D. Long, M. Ponce de Leon, J. T. Matthews, P. G. Spear, M. G. Gibson, L. A. Lasky, P. Berman, E. Golub, and G. H. Cohen.** 1985. Localization of epitopes of herpes simplex virus type 1 glycoprotein D. J. Virol. **53:**634–644.
11. **Evan, G. I., G. K. Lewis, G. Ramsay, and J. M. Bishop.** 1985. Isolation of monoclonal antibodies specific for human c-Myc proto-oncogene product. Mol. Cell. Biol. **5:**3610–3616.
12. **Forrester, A. J., V. Sullivan, A. Simmons, B. A. Blacklaws, G. L. Smith, A. A. Nash, and A. C. Minson.** 1991. Induction of protective immunity with antibody to herpes simplex virus type 1 glycoprotein H (gH) and analysis of the immune response to gH expressed in recombinant vaccinia virus. J. Gen. Virol. **72:**369–375.
13. **Fuller, A. O., and W. C. Lee.** 1992. Herpes simplex virus type 1 entry through a cascade of virus-cell interactions requires different roles of gD and gH in penetration. J. Virol. **66:**5002–5012.
14. **Galdiero, M., A. Whiteley, B. Bruun, S. Bell, T. Minson, and H. Browne.** 1997. Site-directed and linker insertion mutagenesis of herpes simplex virus type 1 glycoprotein H. J. Virol. **71:**2163–2170.
15. **Galdiero, S., A. Falanga, M. Vitiello, H. Browne, C. Pedone, and M. Galdiero.** 2005. Fusogenic domains in herpes simplex virus type 1 glycoprotein H. J. Biol. Chem. **280:**28632–28643.
16. **Gianni, T., P. L. Martelli, R. Casadio, and G. Campadelli-Fiume.** 2005. The ectodomain of herpes simplex virus glycoprotein H contains a membrane alpha-helix with attributes of an internal fusion peptide, positionally conserved in the *Herpesviridae* family. J. Virol. **79:**2931–2940.
17. **Gianni, T., L. Menotti, and G. Campadelli-Fiume.** 2005. A heptad repeat in herpes simplex virus 1 gH, located downstream of the alpha-helix with attributes of a fusion peptide, is critical for virus entry and fusion. J. Virol. **79:**7042–7049.
18. **Gompels, U. A., A. L. Carss, C. Saxby, D. C. Hancock, A. Forrester, and A. C. Minson.** 1991. Characterization and sequence analyses of antibody-selected antigenic variants of herpes simplex virus show a conformationally complex epitope on glycoprotein H. J. Virol. **65:**2393–2401.
19. **Gompels, U. A., and A. C. Minson.** 1989. Antigenic properties and cellular localization of herpes simplex virus glycoprotein H synthesized in a mammalian cell expression system. J. Virol. **63:**4744–4755.
20. **Hutchinson, L., H. Browne, V. Wargent, N. Davis-Poynter, S. Primorac, K. Goldsmith, A. C. Minson, and D. C. Johnson.** 1992. A novel herpes simplex virus glycoprotein, gL, forms a complex with glycoprotein H (gH) and affects normal folding and surface expression of gH. J. Virol. **66:**2240–2250.
21. **Isola, V. J., R. J. Eisenberg, G. R. Siebert, C. J. Heilman, W. C. Wilcox, and G. H. Cohen.** 1989. Fine mapping of antigenic site II of herpes simplex virus glycoprotein D. J. Virol. **63:**2325–2334.
22. **Krummenacher, C., I. Baribaud, M. Ponce de Leon, J. C. Whitbeck, H. Lou, G. H. Cohen, and R. J. Eisenberg.** 2000. Localization of a binding site for herpes simplex virus glycoprotein D on the herpesvirus entry mediator C by using anti-receptor monoclonal antibodies. J. Virol. **74:**10863–10872.
23. **Liu, D. X., U. A. Gompels, L. Foa-Tomasi, and G. Campadelli-Fiume.** 1993. Human herpesvirus-6 glycoprotein H and L homologs are components of the gp100 complex and the gH external domain is the target for neutralizing monoclonal antibodies. Virology **197:**12–22.
24. **Long, D., W. C. Wilcox, W. R. Abrams, G. H. Cohen, and R. J. Eisenberg.** 1992. Disulfide bond structure of glycoprotein D of herpes simplex virus types 1 and 2. J. Virol. **66:**6668–6685.
25. **Lopper, M., and T. Compton.** 2004. Coiled-coil domains in glycoproteins B and H are involved in human cytomegalovirus membrane fusion. J. Virol. **78:**8333–8341.
26. **Miller, N., and L. M. Hutt-Fletcher.** 1988. A monoclonal antibody to glycoprotein gp85 inhibits fusion but not attachment of Epstein-Barr virus. J. Virol. **62:**2366–2372.
27. **Muggeridge, M. I.** 2000. Characterization of cell-cell fusion mediated by herpes simplex virus 2 glycoproteins gB, gD, gH and gL in transfected cells. J. Gen. Virol. **81:**2017–2027.
28. **Naranatt, P., S. Akula, and B. Chandran.** 2002. Characterization of γ2-human herpesvirus-8 glycoproteins gH and gL. Arch. Virol. **147:**1349–1370.
29. **Nicola, A. V., M. Ponce de Leon, R. Xu, W. Hou, J. C. Whitbeck, C. Krummenacher, R. I. Montgomery, P. G. Spear, R. J. Eisenberg, and G. H. Cohen.** 1998. Monoclonal antibodies to distinct sites on the herpes simplex virus (HSV) glycoprotein D block HSV binding to HVEM. J. Virol. **72:**3595–3601.
30. **Novotny, M., M. Parish, and P. Spear.** 1996. Variability of herpes simplex virus 1 gL and anti-gL antibodies that inhibit cell fusion but not viral infectivity. Virology **221:**1–13.
31. **Okuma, K., M. Nakamura, S. Nakano, Y. Niho, and Y. Matsuura.** 1999. Host range of human T-cell leukemia virus type I analyzed by a cell fusion-dependent reporter gene activation assay. Virology **254:**235–244.
32. **Peng, T., M. Ponce de Leon, M. J. Novotny, H. Jiang, J. D. Lambris, G. Dubin, P. G. Spear, R. J. Eisenberg, and G. H. Cohen.** 1998. Structural and antigenic analysis of a truncated form of the herpes simplex virus glycoprotein gH-gL complex. J. Virol. **72:**6092–6103.
33. **Pertel, P. E., A. Fridberg, M. L. Parish, and P. G. Spear.** 2001. Cell fusion induced by herpes simplex virus glycoproteins gB, gD, and gH-gL requires a gD receptor but not necessarily heparan sulfate. Virology **279:**313–324.
34. **Roop, C., L. Hutchinson, and D. C. Johnson.** 1993. A mutant herpes simplex virus type 1 unable to express glycoprotein L cannot enter cells, and its particles lack glycoprotein H. J. Virol. **67:**2285–2297.

35. **Showalter, S. D., M. Zweig, and B. Hampar.** 1981. Monoclonal antibodies to herpes simplex virus type 1 proteins, including the immediate-early protein ICP 4. Infect. Immun. **34:**684–692.
36. **Spear, P. G., R. J. Eisenberg, and G. H. Cohen.** 2000. Three classes of cell surface receptors for alphaherpesvirus entry. Virology **275:**1–8.
37. **Tal-Singer, R., C. Peng, M. Ponce de Leon, W. R. Abrams, B. W. Banfield, F. Tufaro, G. H. Cohen, and R. J. Eisenberg.** 1995. Interaction of herpes simplex virus glycoprotein gC with mammalian cell surface molecules. J. Virol. **69:**4471–4483.
38. **Turner, A., B. Bruun, T. Minson, and H. Browne.** 1998. Glycoproteins gB, gD, and gHgL of herpes simplex virus type 1 are necessary and sufficient to mediate membrane fusion in a Cos cell transfection system. J. Virol. **72:**873–875.
39. **Wang, Z., M. Raifu, M. Howard, L. Smith, D. Hansen, R. Goldsby, and D. Ratner.** 2000. Universal PCR amplification of mouse immunoglobulin gene variable regions: the design of degenerate primers and an assessment of the effect of DNA polymerase 3′ to 5′ exonuclease activity. J. Immunol. Methods **233:**167–177.
40. **Westra, D. F., H. B. Kuiperij, G. W. Welling, A. J. Scheffer, T. H. The, and S. Welling-Wester.** 1999. Domains of glycoprotein H of herpes simplex virus type 1 involved in complex formation with glycoprotein L. Virology **261:**96–105.
41. **Whitbeck, J. C., M. I. Muggeridge, A. Rux, W. Hou, C. Krummenacher, H. Lou, A. van Geelen, R. J. Eisenberg, and G. H. Cohen.** 1999. The major neutralizing antigenic site on herpes simplex virus glycoprotein D overlaps a receptor-binding domain. J. Virol. **73:**9879–9890.